IN-93
84320
P-17

NASA
Technical
Paper
3147

April 1992

An Efficient HZETRN (A Galactic Cosmic Ray Transport Code)

Judy L. Shinn
and John W. Wilson

NASA

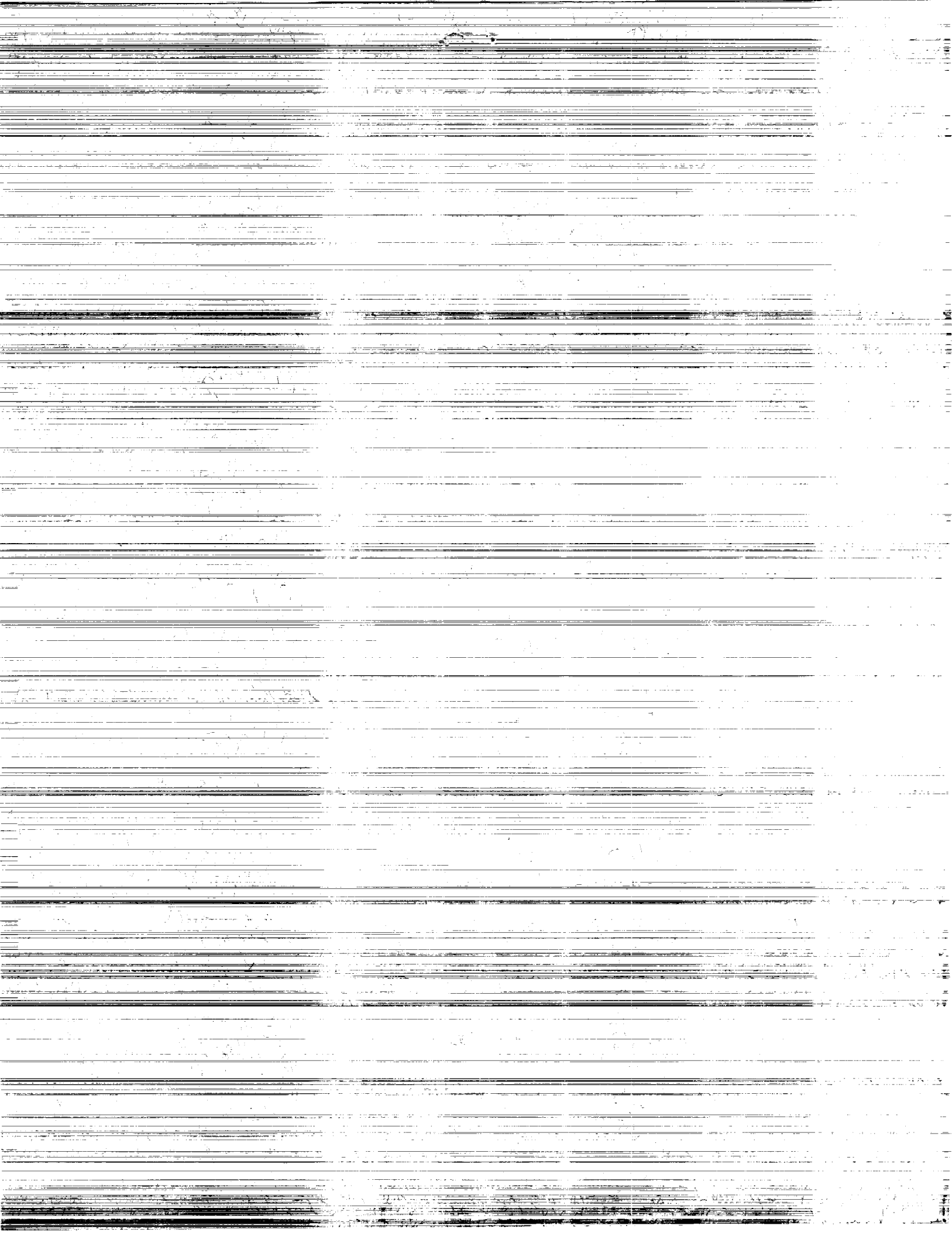

NASA Technical Paper 3147

1992

An Efficient HZETRN (A Galactic Cosmic Ray Transport Code)

Judy L. Shinn
and John W. Wilson
Langley Research Center
Hampton, Virginia

NASA
National Aeronautics and Space Administration
Office of Management
Scientific and Technical Information Program

Abstract

To meet the challenge of the future deep-space program, which involves extended manned space missions, an accurate and efficient engineering code for analyzing the shielding requirement against the high-energy galactic heavy ions is needed. The HZETRN is a deterministic code developed at Langley Research Center that is constantly under improvement both in physics and numerical computation and is targeted for such use. One problem area connected with the space-marching technique used in this code is the propagation of the local truncation error. By improving the numerical algorithms for interpolation, integration, and grid distribution formula, the efficiency of the code is increased by a factor of eight as the number of energy grid points is reduced. The numerical accuracy of better than 2 percent for a shield thickness of 150 g/cm^2 is found when a 45-point energy grid is used. The propagating step size, which is related to the perturbation theory, is also reevaluated.

Introduction

As the space program proceeds into an era of extended manned space operations, the shielding from galactic heavy ions becomes a problem of ever-increasing importance (ref. 1). The high-energy heavy ions originating in deep space interact with target nuclei resulting in energy degradation and nuclear fragmentations. These fragmentations produce secondary and subsequent-generation reaction products that alter the elemental and isotopic composition of the transported radiation fields. A realistic estimate of flux in a critical organ of interest can be made when the nuclear fragmentation data become available as inputs to the galactic cosmic ray transport code (HZETRN (ref. 2)), recently developed at Langley Research Center.

As NASA places efforts on the experimental program to produce fragmentation data, the space radiation transport codes including HZETRN are further being improved, refined, and updated to meet future mission requirements. One such effort is to improve the efficiency and numerical accuracy of these deterministic codes, such that the codes can easily be used as engineering tools and will also accommodate future expansion for more sophistication in physics. Recently, the work on the baryon transport code (BRYNTRN) is an example in this area (ref. 3). This code, as well as HZETRN, is based on a space-marching formalism that calls special attention to the error propagation. An analysis made in the study (ref. 3) showed that the propagated error tends to grow with the marching steps to a maximum, but is proportional to the local error that can be minimized by improving various numerical algorithms and the grid generation. The results of these modifications have substantially improved the accuracy and efficiency of BRYNTRN.

Because HZETRN calculates the transport of the galactic heavy ions through target materials, the number of species and the range of energy considered in this code are much larger than in BRYNTRN. For this reason, the benefit from the improvement of numerical computation in HZETRN is expected to be far greater than in BRYNTRN. In this report, the description and testing of the changes to the computational procedures in HZETRN as well as heavy-ion transport theory are presented. The improvements in efficiency and accuracy are also evaluated.

Galactic Cosmic Ray Transport Method

Galactic Cosmic Ray Transport Theory

In moving through extended matter, heavy ions lose energy through interaction with atomic electrons along their trajectories. On occasion, they interact violently with nuclei of the matter, producing ion fragments moving in the forward direction and low-energy fragments of the struck target nucleus. The transport equations for the short-range target fragments can be solved in closed form in terms of collision density (ref. 4). Hence, the projectile fragment transport is the interesting unsolved problem. In previous work, the projectile ion fragments were treated as if all went straight ahead (ref. 5). The straight-ahead approximation is found to be quite accurate for the nearly isotropic cosmic ray fluence (ref. 4).

With the straight-ahead approximation and the target secondary fragments neglected (refs. 4 and 5), the transport equation may be written as

$$\left[\frac{\partial}{\partial x} - \frac{\partial}{\partial E}\tilde{S}_j(E) + \sigma_j\right]\Phi_j(x,E) = \sum_{k>j} m_{jk}\sigma_k\Phi_k(x,E) \tag{1}$$

where $\Phi_j(x,E)$ is the flux of ions of type j with atomic mass A_j at x moving along the x-axis at energy E in units of MeV/amu, σ_j is the corresponding macroscopic nuclear absorption cross section, $\tilde{S}_j(E)$ is the change in E per unit distance, and m_{jk} is the multiplicity of ion j produced in collision by ion k. The corresponding nucleon transport equation (refs. 3, 6, and 7) is

$$\left[\frac{\partial}{\partial x} - \frac{\partial}{\partial E}\tilde{S}_j(E) + \sigma_j(E)\right]\Phi_j(x,E) = \sum_k \int_E^\infty \sigma_{jk}(E,E')\Phi_k(x,E')\,dE' \tag{2}$$

The m_{jk}, σ_j are assumed energy independent in equation (1) and the full energy dependence is retained in equation (2). The solution to equations (1) and (2) is to be found subject to boundary specification at $x = 0$ and arbitrary E as

$$\Phi_j(0,E) = F_j(E) \tag{3}$$

Usually $F_j(E)$ is called the incident beam spectrum.

It follows from Bethe's theory (ref. 8) that

$$\tilde{S}_j(E) = \frac{A_p Z_j^2}{A_j Z_p^2}\tilde{S}_p(E) \tag{4}$$

and holds for all energies above 100 keV/amu provided the ions remain fully stripped. The range of the ion is given as

$$R_j(E) = \int_0^E \frac{dE'}{\tilde{S}_j(E')} \tag{5}$$

It follows that

$$\frac{Z_j^2}{A_j}R_j(E) = \frac{Z_p^2}{A_p}R_p(E) \tag{6}$$

The subscript p refers to proton. Equation (6) is quite accurate at high energy and only approximately true at low energy because of electron capture by the ion that effectively reduces its charge (ref. 9), higher order Born corrections to Bethe's theory (ref. 10), and nuclear stopping at the lowest energies (refs. 11 and 12). Herein, the parameter ν_j is defined as

$$\nu_j R_j(E) = \nu_k R_k(E) \tag{7}$$

so that

$$\nu_j = Z_j^2/A_j \tag{8}$$

Equations (6) to (8) are used in the subsequent development and the energy variation in ν_j is neglected.

A method of solution is now discussed. For the purpose of solving equation (1), define the coordinates

$$\eta_j \equiv x - R_j(E) \tag{9}$$

$$\xi_j \equiv x + R_j(E) \tag{10}$$

where η_j varies along the particle path and ξ_j is constant along the particle trajectory. The new fluence functions are taken as

$$\chi_j(\eta_j, \xi_j) \equiv \tilde{S}_j(E)\phi_j(x, E) = \psi_j(x, r_j) \tag{11}$$

$$\bar{\chi}_k(\eta_j, \xi_j) \equiv \chi_k(\eta_k, \xi_k) \tag{12}$$

where

$$\xi_j + \eta_j = \xi_k + \eta_k \tag{13}$$

$$\eta_j - \xi_j = \frac{\nu_k}{\nu_j}(\eta_k - \xi_k) \tag{14}$$

and $r_j = R_j(E)$. Under this coordinate mapping, equation (1) becomes

$$\left[2\frac{\partial}{\partial \eta_j} + \sigma_j\right] \chi_j(\eta_j, \xi_j) = \sum_k m_{jk}\sigma_k \, \frac{\nu_j}{\nu_k} \, \bar{\chi}_k(\eta_j, \xi_j) \tag{15}$$

where σ_j are assumed to be energy independent. There is a small variation in σ_j ($\approx$20 percent), which must eventually be taken into account. Solving equation (15) by using line integration with an integrating factor

$$\mu_j(\eta_j, \xi_j) = \exp\left[\frac{1}{2}\,\sigma_j(\xi_j + \eta_j)\right] \tag{16}$$

results in

$$\begin{aligned}\chi_j(\eta_j, \xi_j) = {} & \exp\left[-\frac{1}{2}\,\sigma_j(\xi_j + \eta_j)\right] \, \chi_j(-\xi_j, \xi_j) \\ & + \frac{1}{2}\int_{-\xi_j}^{\eta_j} \exp\left[\frac{1}{2}\,\sigma_j(\eta' - \eta_j)\right] \sum_k \, m_{jk}\sigma_k \, \frac{\nu_j}{\nu_k} \, \chi_k(\eta_k', \xi_k') \, d\eta'\end{aligned} \tag{17}$$

where

$$\eta_k' = \frac{\nu_k + \nu_j}{2\nu_k}\eta' + \frac{\nu_k - \nu_j}{2\nu_k}\xi_j \text{ and } \xi_k' = \frac{\nu_k - \nu_j}{2\nu_k}\eta' + \frac{\nu_k + \nu_j}{2\nu_k}\xi_j$$

With equation (11) one may show

$$\psi_j(x, r_j) = e^{-\sigma_j x} \, \psi_j(0, r_j + x) + \int_0^x dz \, e^{-\sigma_j z} \sum_k \, m_{jk}\sigma_k \, \frac{\nu_j}{\nu_k} \, \psi_k\left(x - z, r_k + \frac{\nu_j}{\nu_k}z\right) \tag{18}$$

Furthermore, it is easy to show that

$$\psi_j(x + h, r_j) = e^{-\sigma_j h} \, \psi_j(x, r_j + h) + \int_0^h dz \, e^{-\sigma_j z} \sum_k \, m_{jk}\sigma_k \, \frac{\nu_j}{\nu_k} \, \psi_k\left(x + h - z, r_k + \frac{\nu_j}{\nu_k}z\right) \tag{19}$$

where h is the step size in the x direction.

It is clear from equation (18) that

$$\psi_k(x + h - z, r_k) = e^{-\sigma_k(h-z)} \, \psi_k(x, r_k + h) + O(h - z) \tag{20}$$

which upon substitution into equation (19) yields

$$\psi_j(x + h, r_j) = e^{-\sigma_j h} \, \psi_j(x, r_j + h) + \int_0^h dz \, e^{-\sigma_j z} \, \sum_k \, m_{jk} \, \sigma_k \, \frac{\nu_j}{\nu_k} \, e^{-\sigma_k(h-z)} \, \psi_k\left(x, r_k + \frac{\nu_j}{\nu_k}z + h - z\right) \tag{21}$$

which is correct to order h^2. This expression may be further approximated by

$$\psi_j(x+h,r_j) = e^{-\sigma_j h}\ \psi_j(x,r_j+h) + \sum_k\ m_{jk}\ \sigma_k\ \frac{\nu_j}{\nu_k}\ \left(\frac{e^{-\sigma_j h} - e^{-\sigma_k h}}{\sigma_k - \sigma_j}\right) \psi_k\left(x, r_k + \frac{\nu_j}{\nu_k} h\right) \tag{22}$$

which is accurate to $O[(\nu_k - \nu_j)h]$. Equation (22) is the basis of the galactic cosmic ray (GCR) transport code GCRTRN (refs. 13 to 15). A few years ago, GCRTRN and the baryon transport code (BRYNTRN) were coupled together as a new code (HZETRN) which effectively solves equation (2) by adding a heavy ion collision source of nucleons to the right-hand side of the equation. Equation (22) provides the propagating algorithm for the heavy ions. The corresponding propagating procedure for the nucleons is given as (refs. 3 and 6)

$$\psi(x+h,r) \approx e^{-\sigma h}\psi(x,r+h) + e^{-\sigma h}\int_0^h dz \int_r^\infty dr' \bar{f}(r+z,r'+z)\ \psi(x,r'+h) \tag{23}$$

with the order of h^2.

There are several quantities of interest that are now given. The integral fluence is given as

$$\phi_j(x,>E) = \int_{R_j(E)}^\infty \psi_j(x,r)\ dr \tag{24}$$

The energy absorption per gram is

$$D_j(x,>E) = \int_E^\infty\ A_j\psi_j[x,R_j(E)]\ dE \tag{25}$$

with the dose equivalent given as

$$H_j(x,>E) = A_j \int_E^\infty\ Q_F\psi_j[x,R_j(E)]\ dE \tag{26}$$

where Q_F is the quality factor. These quantities are used in shield design studies for protection against galactic cosmic rays.

Numerical Procedure

The secondary particle production term of the propagation algorithm for nucleons in equation (23) has been further reduced to a form that can be implemented with ease for numerical integration. The details of the form and its validity have been discussed elsewhere (ref. 6) and will not be repeated here. For the heavy ions, the secondary production term (the second term on the right side of eq. (22)) does not involve any integration; however, the interpolation of the transformed fluence function is based on the independent variable r_k, which is different from r_j, the range of ions of type j given at the left side of the equation. To circumvent the problem, the equation is further modified. Recall the definition of $\tilde{S}_j(E)$ with E given in units of MeV/amu

$$\tilde{S}_j(E) = \tilde{S}_j(E_j/A_j) = -\frac{\Delta(E_j/A_j)}{\Delta x} = -\frac{1}{A_j}\frac{\Delta E_j}{\Delta x} = \frac{1}{A_j}S_j(E_j) \tag{27}$$

with

$$S_j(E_j) = Z_j^2\ S_p(E_j/A_j) \tag{28}$$

where S_p is the proton stopping power and E_j is the energy in MeV of ions of type j. It follows that

$$\tilde{S}_j(E) = \frac{1}{A_j}Z_j^2\ S_p(E_j/A_j) \equiv \nu_j S_p(E_p) \tag{29}$$

where

$$E_p = E_j/A_j \tag{30}$$

Rewriting equation (11) as

$$\psi_j(x, r_j) \equiv \tilde{S}_j(E)\ \phi_j(x, E) = \nu_j\ S_p(E)\ \phi_j(x, E) \tag{31}$$

we can define the new fluence function

$$\psi'_j(x, r) \equiv \nu_j\ S_p(E)\ \phi(x, E) \equiv \psi_j(x, r_j) \tag{32}$$

with $r = r_p = \nu_j\ r_j$, where

$$r_p = \int_0^E \frac{dE'}{S_p(E')} \tag{33}$$

Equation (22) now becomes

$$\psi'_j(x + h, r) = e^{-\sigma_j h}\ \psi'_j(x, r + \nu_j h) + \sum_k\ m_{jk}\ \sigma_k \left(\frac{e^{-\sigma_j h} - e^{-\sigma_k h}}{\sigma_k - \sigma_j} \right) \frac{\nu_k}{\nu_j}\ \psi'_k(x, r + \nu_j h) \tag{34}$$

so that there is only one single definition of range that is related to energy. The equation can now be solved by setting up the r (proton range) grid and marching the solution from $x = 0$ by steps of h to the desired thickness.

Error Propagation

In considering how errors are propagated in the use of equation (34), the error is introduced locally by calculating $\psi'_j(x, r + \nu_j h)$ over the range (energy) grid. Limiting our current analysis to the first term of equation (34), it is defined at each range grid r_i that

$$\psi'_j(x + h, r_i) = e^{-\sigma_j h}\ \psi'_j(x, r_i + \nu_j h) \tag{35}$$

We denote the truncation error ϵ_i introduced in the interpolation procedure to the interpolated value, $\psi'_{j\text{int}}$, as

$$\psi'_j(x, r_i + \nu_j h) = \psi'_{j\text{int}}(x, r_i + \nu_j h) + \epsilon_i(h) \tag{36}$$

After the mth step from the boundary the numerical solution is

$$\psi'_j(mh, r_i) = e^{-\sigma_j h}\ \psi'_{j\text{int}}\left[(m-1)h, r_i + \nu_j h\right] + \sum_{\ell=0}^{m-1}\ e^{-\sigma_j (m-\ell)h} \epsilon_\ell(h) \tag{37}$$

Suppose $0 \le \epsilon_\ell(h) \le \epsilon(h)$ for all ℓ then the propagated error is bound by

$$\epsilon_{\text{prp}}(m) = \sum_{\ell=0}^{m-1}\ e^{-\sigma_j (m-\ell)h} \epsilon_\ell(h) \le \epsilon(h) \sum_{\ell=0}^{m-1}\ e^{-\sigma_j (m-\ell)h} \tag{38}$$

We note that

$$\sum_{\ell=0}^{m-1} e^{-\sigma_j mh}\ e^{\sigma_j h\ell} \approx \frac{1}{h\sigma_j} \left[1 - e^{-\sigma_j mh}\right] \tag{39}$$

because $h\sigma_j \ll 1$. Clearly the propagated error on the mth step is bound by

$$\epsilon_{\text{prp}}(h) < \frac{\epsilon(h)}{h\sigma_j} \left[1 - e^{-\sigma_j mh}\right] \tag{40}$$

where $\epsilon(h)$ is the maximum error per step. With the increasing value of m, the propagated error grows each step to a maximum value of $\epsilon(h)/h\sigma_j$. Because the increase of h value is limited by the perturbation theory, reducing the local truncation error is the only viable approach left for reducing the propagated error to a desired level. The same consideration may be applied for the second term of equation (34), as the terms are of similar nature.

Numerical Algorithms

The error analysis shown in the previous section has concluded that to effectively reduce the level of propagated error, the local truncated error must be reduced. There are three basic numerical algorithms that are involved in solving equations (23) to (26) and (34): interpolation, integration, and grid generation. The integration scheme does not affect the error propagation for the heavy-ion transport, but does affect the nucleons and the dose calculations. The choice of a grid distribution that is interrelated to the interpolation and integration scheme can increase the efficiency of the code if the number of grids can be reduced.

The interpolation scheme to be used here is the third-order Lagrange method as used successfully in the work for improving BRYNTRN (ref. 3). With the four neighboring interpolating grids (data points) placed evenly on both sides of the interpolated point, the error will tend to be the smallest in the middle interval of all the data points if the grid distribution is rather uniform (ref. 16). The choice of a much higher order Lagrange method will substantially decrease the efficiency of the code, because there are more than 10 interpolation calls for each single energy point at each step. Other interpolation methods such as a cubic spline were considered but discarded. The splines are, in general, more accurate. However, their characteristic large excursions (oscillations) can result in erroneous, unpredictable solutions.

The same procedure for numerical integration used for the improved BRYNTRN (ref. 3) will also be used here for HZETRN. It is based on the compound quadrature formulation summing over all the subintervals between the grids with the midpoint evaluated by making use of the improved interpolation procedure mentioned above. A simple numerical method such as Simpson's rule is used to integrate for the subintervals.

There are three binding conditions that dictate how the grids should be distributed. The first is the shape of the input spectrum. Because the galactic cosmic ray fluences are several orders of magnitude larger at the lower energy end (ref. 17), the logarithmic scale will be used for the energy or range coordinate as was done in reference 3. The second condition is related to the choice of the interpolation method that requires the four neighboring grids to be as uniformly spaced (on logarithm scale) as possible so that the interpolation error can be minimized. Because the interpolation is performed on the range grid rather than on the energy grid, a uniform grid distribution on a logarithm of range r is desired. The third is related to the efficiency of the code that is found to increase almost quadratically with the decrease of grid points. With the uniform grid points on logarithm r scale as the basic structure, the distribution can further be modified to reduce the number of points in the region in which the information is not propagating through the steps. For BRYNTRN, it is the region below $r_{\min} + h$, or approximately 1 g/cm^2 because $r_{\min} \ll 1$ and assuming $h = 1$ g/cm^2 (ref. 3). The same applies for HZETRN, although the interpolation is now at $r_{\min} + \nu_j h$, where ν_j is always equal to or much greater than 1.

Results and Discussion

In a previous study (ref. 3), the new grid distribution with the number of grid points N equals 30 was found satisfactory for BRYNTRN, with the calculated dose of 5 percent accuracy for a shield thickness of 150 g/cm^2. Because the galactic cosmic rays are much harder than the solar flare protons, the upper limit of the energy range is usually taken to be about 50 GeV as compared with a few GeV for solar protons. Thus, more grid points are used for HZETRN. Tests were performed to determine the differences between the interpolated $\psi'_k(0,\ r+\nu_j h)$ and the analytical results using the new interpolation method and grid distribution with $N = 45$, for all the j's and k's where $j < k$. Samples of the results are displayed in figures 1 to 6. The overall error has been found to be less than 0.2 percent, with the particular grid generation formula purposely adjusted so that the larger errors are absorbed at the low-energy region for r less than $r_{\min} + \nu_j h$, where $h = 1$ g/cm^2. The errors reported here are far less than the interpolation error reported in reference 3 for BRYNTRN.

To test the convergence of the solution from the improved HZETRN (including the new integration procedure), the absorbed doses in tissue behind various thicknesses of aluminum shield exposed to the galactic cosmic rays at solar minimum are calculated with $N = 45$, 60, and 90. The shield thickness is varied up to 150 g/cm^2 as indicated in figure 7. The doses from the heavy ions decrease significantly through the shield as they are fragmented by the

target nuclei. The doses from the nucleons increase rapidly to a maximum as a result of such fragmentation and then gradually decrease. The relative errors in the absorbed dose for 45 grids or 60 grids compared with the dose for 90 grids are plotted in figures 8(a) and 8(b). The error for the proton dose increases with the shield thickness (see fig. 8(a)) as was expected from the analysis of error propagation. There is some indication of oscillation for the neutron component (see fig. 8(b)), which was pointed out earlier (ref. 3) to be the result of the rapidly varying cross-section data for neutrons at low energy. The errors for the other component are found to be insignificant compared with those for the nucleons. Thus, the maximum error is 2 percent for 45 grids and decreases to less than 1 percent for 60 grids, showing good convergence.

Another convergence issue that needs to be addressed is the perturbation theory used in the transport theory. The perturbation theory requires $\sigma_j h \ll 1$. Because σ_j is on the order of 0.01, we usually take $h = 1$ g/cm^2. Table 1 shows the effect of step size on some of the calculated doses, with $h = 0.5$ and 1 g/cm^2. The differences between these two step sizes are insignificantly small, therefore, $h = 1$ g/cm^2 is retained for HZETRN. The overall efficiency for this code is improved about eight times as the grid points are reduced from 160 to 45, with an accuracy of 2 percent for the large shield thickness. A typical run time for producing the results shown in figure 7 is about 5000 sec on a CYBER 800 series computer.

Concluding Remarks

The efficiency of HZETRN (a galactic cosmic ray transport code) has been improved by approximately a factor of eight. The numerical algorithms for interpolation, integration, and energy grid generation were modified such that the number of grid points needed was reduced from 160 to 45 points. The error in dose calculation for 45 grid points was determined to be within 2 percent by a convergence test. The adequacy of the step size, which is related to the perturbation theory, was also examined.

NASA Langley Research Center
Hampton, VA 23665-5225
February 4, 1992

References

1. Grahn, Douglas, ed.: *HZE-Particle Effects in Manned Spaceflight.* National Academy of Sciences, 1973.

2. Wilson, John W.; Chun, S. Y.; Badavi, F. F.; Townsend, Lawrence W.; and Lamkin, S. L.: *HZETRN: A Heavy Ion/Nucleon Transport Code for Space Radiations.* NASA TP-3146, 1991.

3. Shinn, Judy L.; Wilson, John W.; Weyland, Mark; and Cucinotta, Francis A.: *Improvements in Computational Accuracy of BRYNTRN (A Baryon Transport Code).* NASA TP-3093, 1991.

4. Wilson, John W.: *Analysis of the Theory of High-Energy Ion Transport.* NASA TN D-8381, 1977.

5. Wilson, John W.: *Heavy Ion Transport in the Straight Ahead Approximation.* NASA TP-2178, 1983.

6. Wilson, John W.; Townsend, Lawrence W.; Nealy, John E.; Chun, Sang Y.; Hong, B. S.; Buck, Warren W.; Lamkin, S. L.; Ganapol, Barry D.; Khan, Ferdous; and Cucinotta, Francis A.: *BRYNTRN: A Baryon Transport Model.* NASA TP-2887, 1989.

7. Shinn, Judy L.; Wilson, John W.; Nealy, John E.; and Cucinotta, Francis A.: *Comparison of Dose Estimates Using the Buildup-Factor Method and a Baryon Transport Code (BRYNTRN) With Monte Carlo Results.* NASA TP-3021, 1990.

8. Bethe, H.: Zur Theorie des Durchgangs schneller Korpuskularstrahlen durch Materie. *Ann. Phys.*, 5 Folge, Bd. 5, 1930, pp. 325–400.

9. Janni, Joseph F.: *Calculations of Energy Loss, Range, Pathlength, Straggling, Multiple Scattering, and the Probability of Inelastic Nuclear Collisions for 0.1- to 1000-MeV Protons.* AFWL-TR-65-150, U.S. Air Force, Sept. 1966. (Available from DTIC as AD 643 837.)

10. Andersen, H. H.; Simonsen, H.; and Sorensen, H.: An Experimental Investigation of Charge-Dependent Deviations From the Bethe Stopping Power Formula. *Nucl. Phys.*, vol. A125, no. 1, Feb. 24, 1969, pp. 171–175.

11. Lindhard, J.; Scharff, M.; and Schiott, H. E.: Range Concepts and Heavy Ion Ranges (Notes on Atomic Collisions, II). *Mat.-Fys. Medd. - K. Dan. Videnske. Selsk.*, vol. 33, no. 14, 1963, pp. 1–42.

12. Ziegler, J. F.: *Handbook of Stopping Cross-Sections for Energetic Ions in All Elements.* Volume 5 of *The Stopping and Ranges of Ions in Matter*, J. F. Ziegler, ed., Pergamon Press, Inc., c.1980.

13. Wilson, John W.; and Badavi, F. F.: Methods of Galactic Heavy Ion Transport. *Radiat. Res.*, vol. 108, 1986, pp. 231–237.

14. Wilson, John W.; Townsend, Lawrence W.; and Badavi, Forooz F.: Galactic HZE Propagation Through the Earth's Atmosphere. *Radiat. Res.,* vol. 109, no. 2, Feb. 1987, pp. 173–183.

15. Wilson, John W.; and Townsend, L. W.: A Benchmark for Galactic Cosmic-Ray Transport Codes. *Radiat. Res.,* vol. 114, no. 2, May 1988, pp. 201–206.

16. Yakowitz, Sidney; and Szidarovszky, Ferenc: *An Introduction to Numerical Computations,* Second ed. Macmillan Publ. Co., c.1989.

17. Adams, J. H., Jr.; Silberberg, R.; and Tsao, C. H.: *Cosmic Ray Effects on Microelectronics. Part I– The Near-Earth Particle Environment.* NRL Memo. Rep. 4506-Pt. I, U.S. Navy, Aug. 1981. (Available from DTIC as AD A103 897.)

Table 1. Effect of Step Size on Calculated Doses Through Various Thicknesses of Aluminum Shield

Aluminum shield thickness, g/cm^2	Neutron dose, Gy		Proton dose, Gy		Alpha particle dose, Gy	
	Step size = 0.5 g/cm^2	Step size = 1 g/cm^2	Step size = 0.5 g/cm^2	Step size = 1 g/cm^2	Step size = 0.5 g/cm^2	Step size = 1 g/cm^2
5	6.3599E-3	6.3315E-3	8.2623E-2	8.2375E-2	2.4349E-2	2.4349E-2
10	1.1232E-2	1.1181E-2	9.1011E-2	9.0682E-2	2.1400E-2	2.1400E-2
15	1.4942E-2	1.4873E-2	9.4520E-2	9.4148E-2	1.8784E-2	1.8784E-2
20	1.7738E-2	1.7655E-2	9.5463E-2	9.5068E-2	1.6499E-2	1.6499E-2

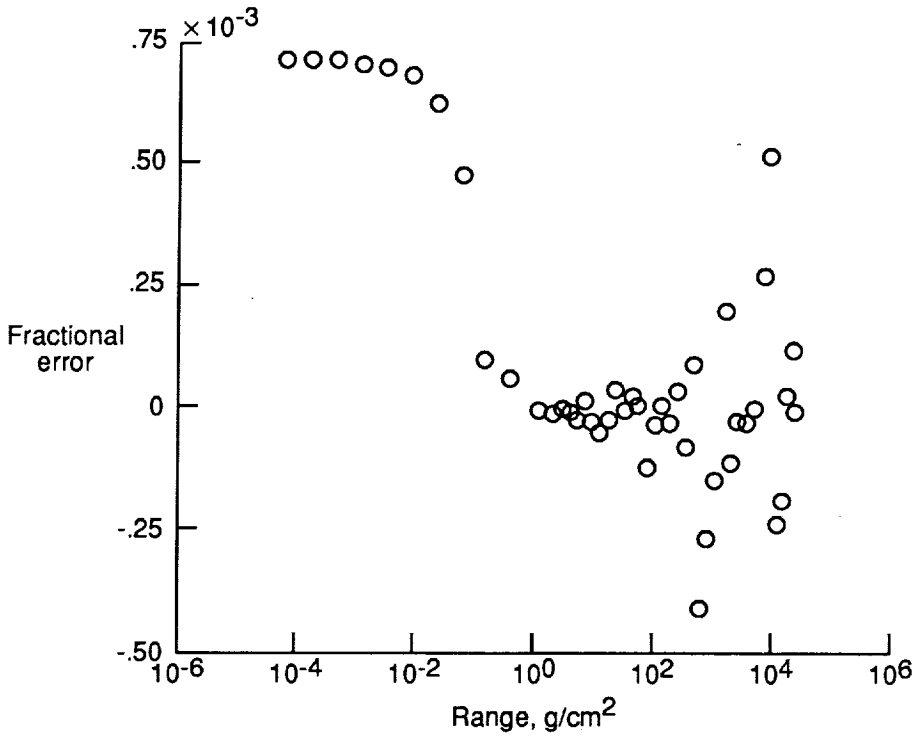

Figure 1. Fractional error of interpolating alpha-particle component of GCR spectrum at solar minimum with new grid distribution and interpolation method for generation of secondary alpha-particles.

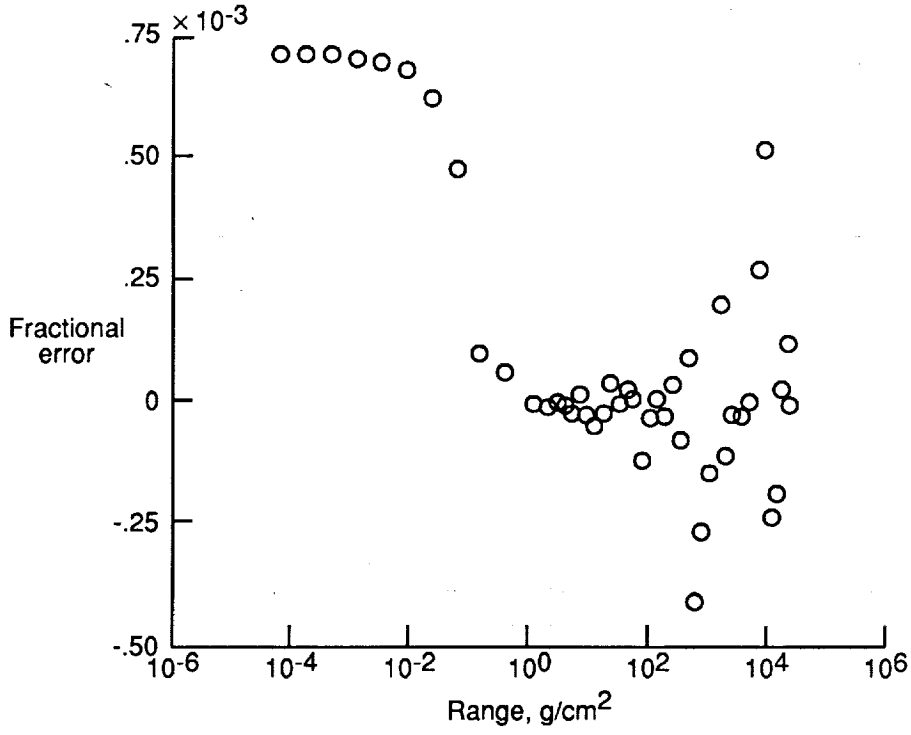

Figure 2. Fractional error of interpolating phosphorus component of GCR spectrum at solar minimum with new grid distribution and interpolation method for generation of secondary alpha-particles.

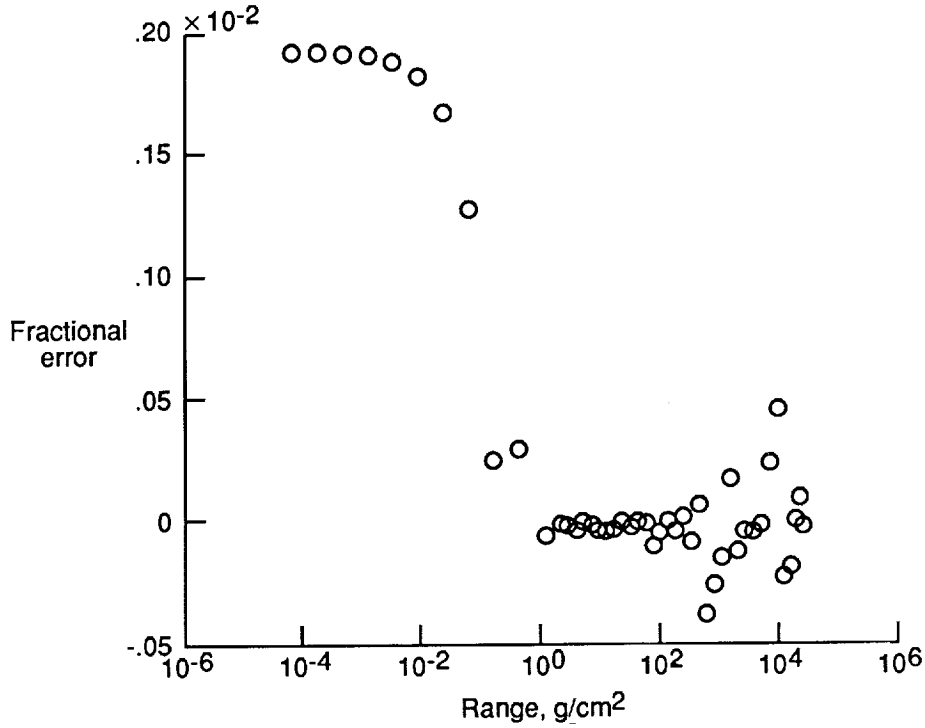

Figure 3. Fractional error of interpolating nickel component of GCR spectrum at solar minimum with new grid distribution and interpolation method for generation of secondary alpha-particles.

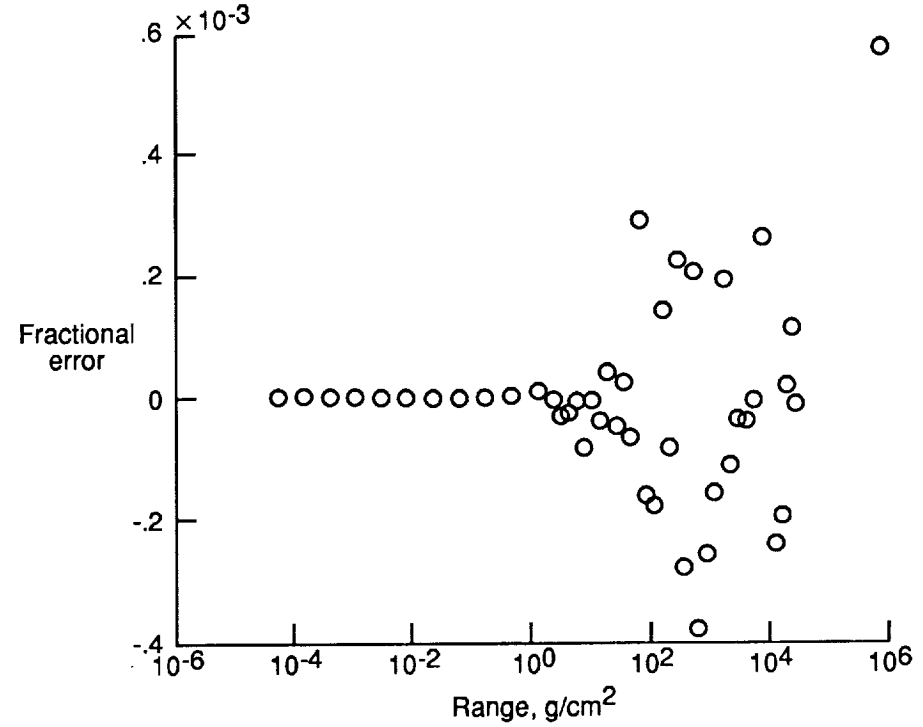

Figure 4. Fractional error of interpolating phosphorus component of GCR spectrum at solar minimum with new grid distribution and interpolation method for generation of secondary phosphorus.

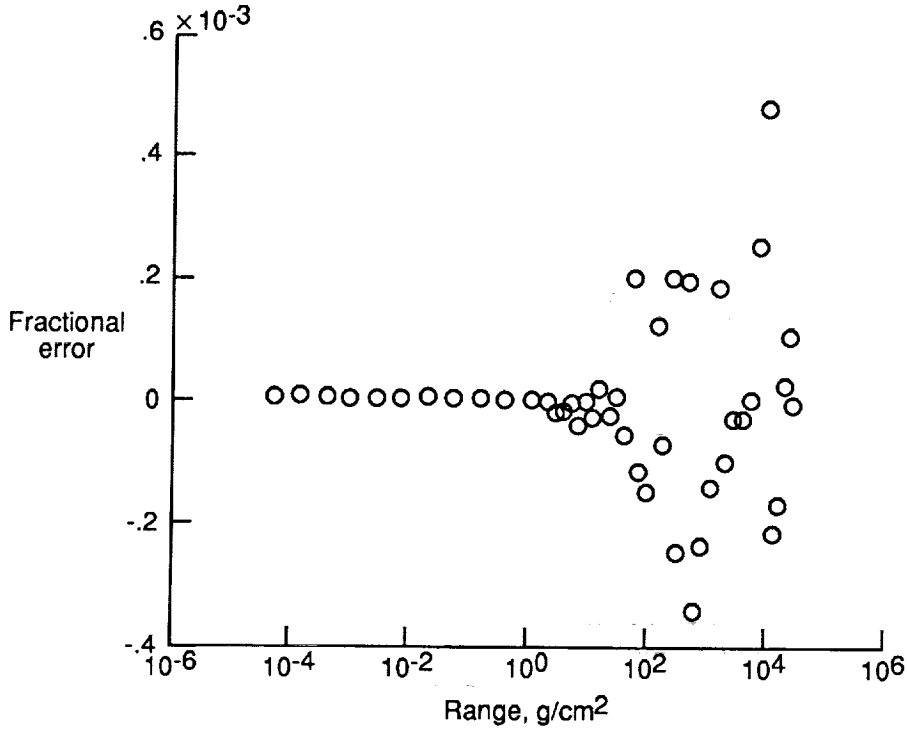

Figure 5. Fractional error in interpolating nickel component of GCR spectrum at solar minimum with new grid distribution and interpolation method for generation of secondary phosphorus.

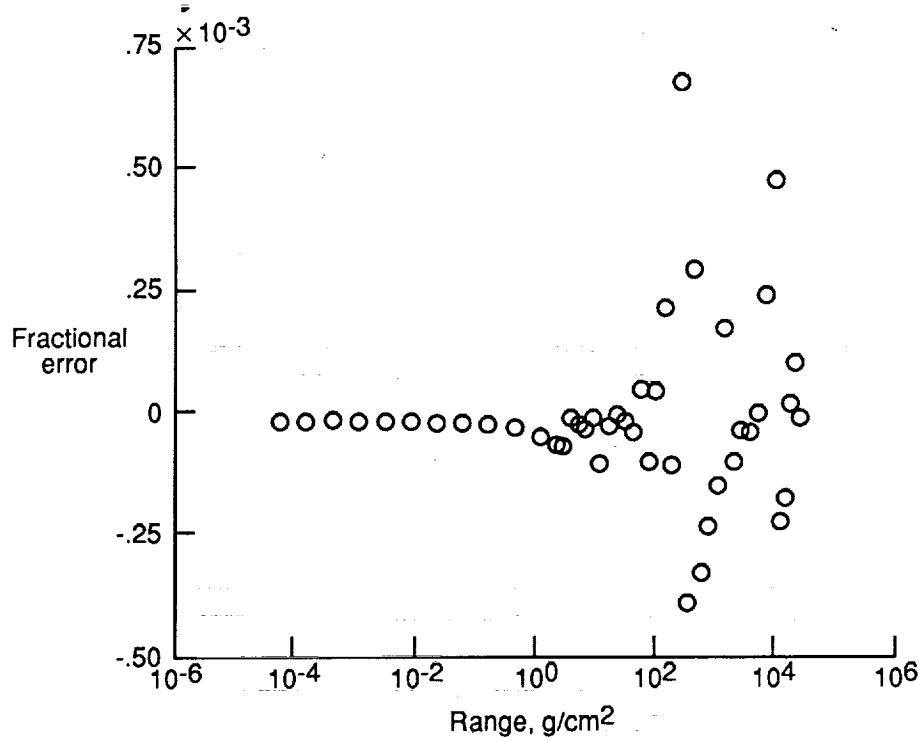

Figure 6. Fractional error in interpolating nickel component of GCR spectrum at solar minimum with new grid distribution and interpolation method for generation of secondary nickel.

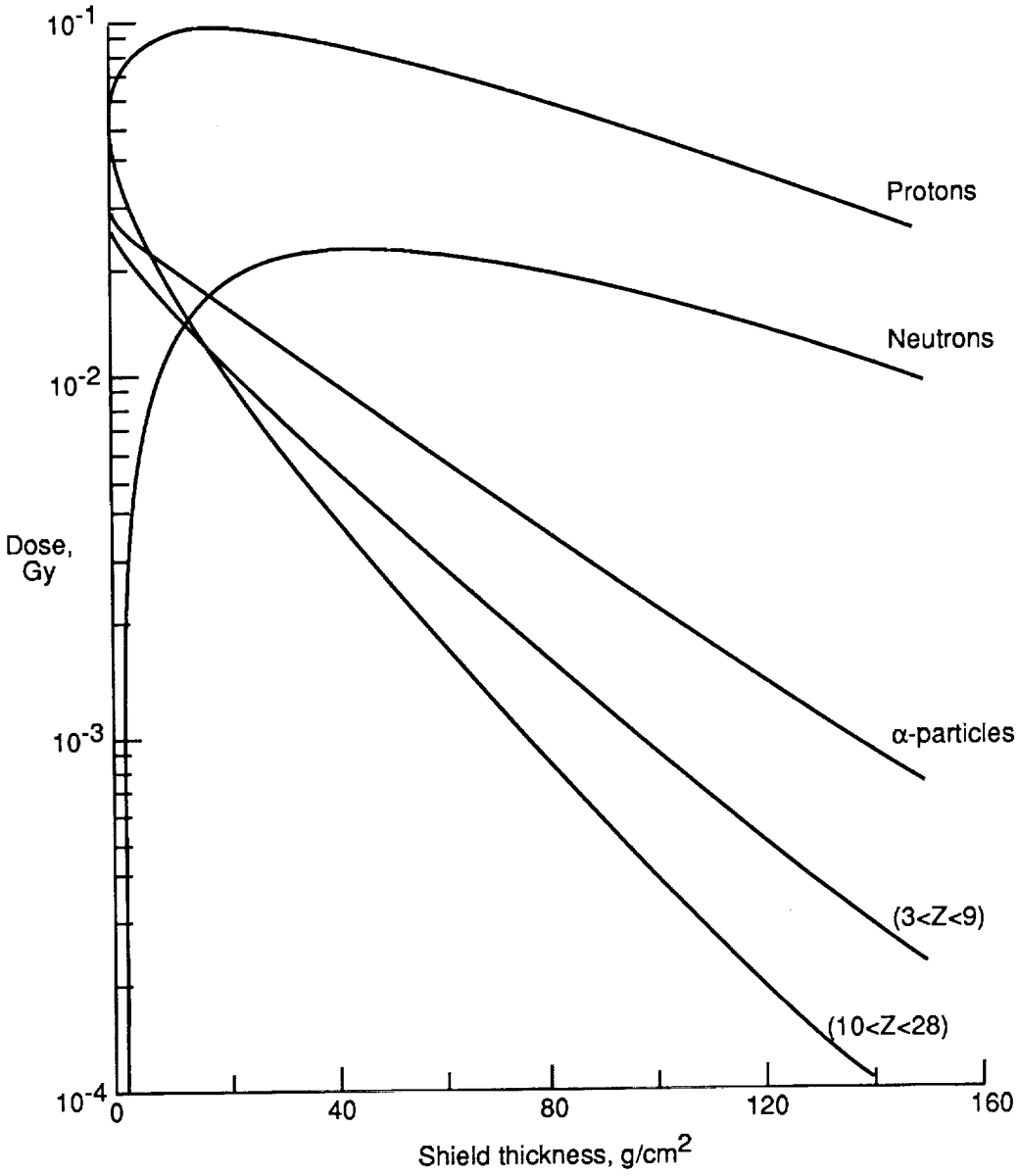

Figure 7. Calculated absorbed dose components in tissue as function of aluminum shield thickness exposed to GCR at solar minimum.

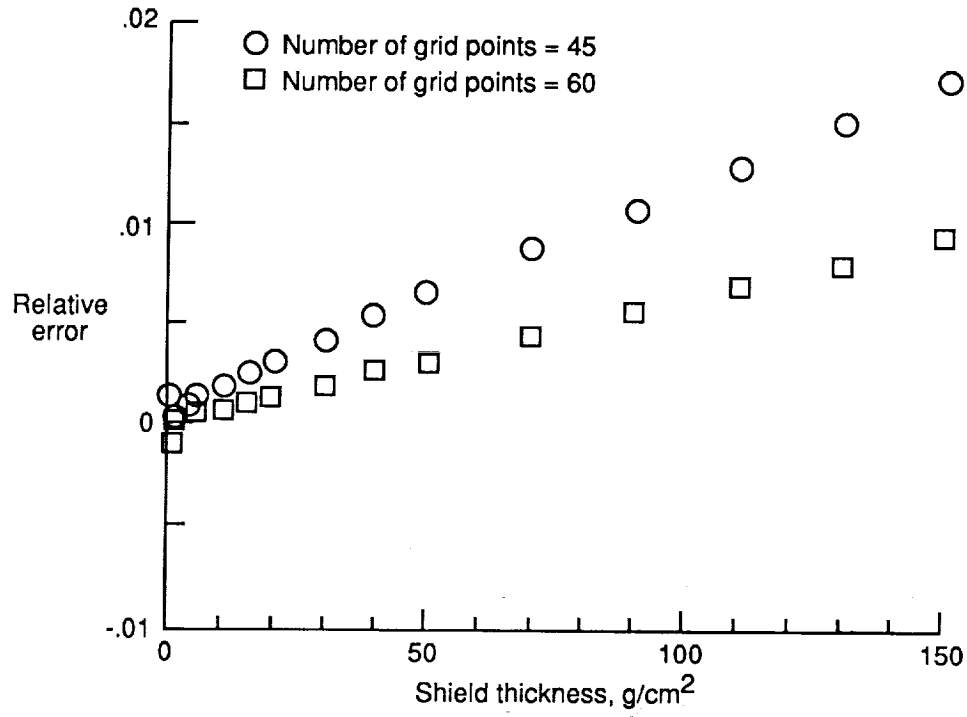

(a) Proton dose.

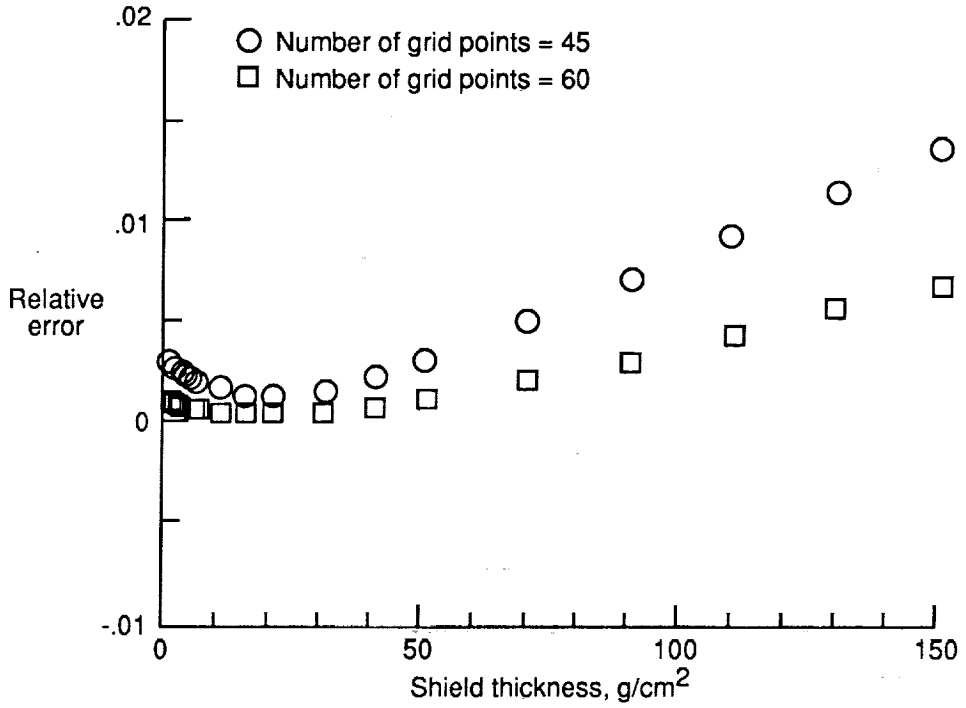

(b) Neutron dose.

Figure 8. Relative errors in doses compared with those calculated with 90 grid points. Doses are same as in figure 7.

REPORT DOCUMENTATION PAGE

Form Approved
OMB No. 0704-0188

1. AGENCY USE ONLY *(Leave blank)*	2. REPORT DATE	3. REPORT TYPE AND DATES COVERED
	April 1992	Technical Paper

4. TITLE AND SUBTITLE
An Efficient HZETRN (A Galactic Cosmic Ray Transport Code)

5. FUNDING NUMBERS
WU 593-42-21

6. AUTHOR(S)
Judy L. Shinn and John W. Wilson

7. PERFORMING ORGANIZATION NAME(S) AND ADDRESS(ES)
NASA Langley Research Center
Hampton, VA 23665-5225

8. PERFORMING ORGANIZATION REPORT NUMBER
L-16954

9. SPONSORING/MONITORING AGENCY NAME(S) AND ADDRESS(ES)
National Aeronautics and Space Administration
Washington, DC 20546-0001

10. SPONSORING/MONITORING AGENCY REPORT NUMBER
NASA TP-3147

11. SUPPLEMENTARY NOTES

12a. DISTRIBUTION/AVAILABILITY STATEMENT
Unclassified Unlimited

Subject Category 93

12b. DISTRIBUTION CODE

13. ABSTRACT *(Maximum 200 words)*

To meet the challenge of the future deep-space program, which involves extended manned space missions, an accurate and efficient engineering code for analyzing the shielding requirement against the high-energy galactic heavy ions is needed. The HZETRN is a deterministic code developed at Langley Research Center that is constantly under improvement both in physics and numerical computation and is targeted for such use. One problem area connected with the space-marching technique used in this code is the propagation of the local truncation error. By improving the numerical algorithms for interpolation, integration, and grid distribution formula, the efficiency of the code is increased by a factor of eight as the number of energy grid points is reduced. The numerical accuracy of better than 2 percent for a shield thickness of 150 g/cm^2 is found when a 45-point energy grid is used. The propagating step size, which is related to the perturbation theory, is also reevaluated.

14. SUBJECT TERMS	15. NUMBER OF PAGES
Space radiation; Numerical accuracy; High-energy transport	15
	16. PRICE CODE: A03

17. SECURITY CLASSIFICATION OF REPORT	18. SECURITY CLASSIFICATION OF THIS PAGE	19. SECURITY CLASSIFICATION OF ABSTRACT	20. LIMITATION OF ABSTRACT
Unclassified	Unclassified		

NSN 7540-01-280-5500

Standard Form 298(Rev. 2-89)
Prescribed by ANSI Std. Z39-18
298-102

NASA-Langley, 1992